Targeting CLEC9A delivers antigen to human CD141+ DC for CD4+ and CD8+ T cell recognition

Kirsteen M. Tullett,[1,2,3,4] Ingrid M. Leal Rojas,[1] Yoshihito Minoda,[1,5] Peck S. Tan,[3,4]
Jian-Guo Zhang,[6,7] Corey Smith,[8] Rajiv Khanna,[8] Ken Shortman,[6,7] Irina Caminschi,[3,4,9]
Mireille H. Lahoud,[3,4] Kristen J. Radford[1,5]

[1]Mater Research Institute - University of Queensland, Translational Research Institute, Brisbane, Queensland, Australia.
[2]University of Queensland, School of Medicine, Brisbane, Queensland, Australia. [3]Infection and Immunity Program,
Monash Biomedicine Discovery Institute and Department of Biochemistry and Molecular Biology, Monash University,
Melbourne, Victoria, Australia. [4]Centre for Biomedical Research, Burnet Institute, Melbourne, Victoria, Australia.
[5]University of Queensland, School of Biomedical Sciences, Brisbane, Queensland, Australia. [6]The Walter and Eliza Hall
Institute of Medical Research, Parkville, Victoria, Australia. [7]Department of Medical Biology, The University of Melbourne,
Parkville, Victoria, Australia. [8]QIMR Berghofer Medical Research Institute, Brisbane, Queensland, Australia. [9]Department
of Microbiology and Immunology, The University of Melbourne, Parkville, Victoria, Australia.

DC-based vaccines that initiate T cell responses are well tolerated and have demonstrated efficacy for tumor immunotherapy, with the potential to be combined with other therapies. Targeting vaccine antigens (Ag) directly to the DCs in vivo is more effective than cell-based therapies in mouse models and is therefore a promising strategy to translate to humans. The human CD141+ DCs are considered the most clinically relevant for initiating CD8+ T cell responses critical for killing tumors or infected cells, and they specifically express the C-type lectin-like receptor CLEC9A that facilitates presentation of Ag by these DCs. We have therefore developed a human chimeric Ab that specifically targets CLEC9A on CD141+ DCs in vitro and in vivo. These human chimeric Abs are highly effective at delivering Ag to DCs for recognition by both CD4+ and CD8+ T cells. Given the importance of these cellular responses for antitumor or antiviral immunity, and the superior specificity of anti-CLEC9A Abs for this DC subset, this approach warrants further development for vaccines.

Introduction

The induction of CD8+ cytotoxic T cells (CTLs) is important for protective immunity against cancer and many pathogens for which there are no effective vaccines. DCs are professional antigen-presenting (Ag-presenting) cells that initiate and direct immune responses, including CTLs. This property has led to their exploitation as immunotherapeutic vaccines (1). The development of Ab-based vaccines designed to target DCs in vivo, specifically the key DC subtype responsible for CTL induction, is a promising approach to overcome many of the limitations of cellular vaccines.

Human DCs can be found in lymphoid and nonlymphoid tissues in the steady state and are classically defined as leukocytes that express HLA-DR and lack expression of lineage markers. They can be further classified into 3 major subsets: the CLEC4C+CD123+CD11c− plasmacytoid DCs, the CD141+CLEC9A+XCR1+ DCs (also known as cDC1), and the CD1c+CD11b+CD11c+ DCs (cDC2) (1, 2). Transcriptome and functional analysis has aligned human CD141+ DCs with the mouse CD8α+ lymphoid tissue DCs and their CD103+ nonlymphoid tissue equivalents (3, 4). Mouse CD8α+/CD103+ DCs are essential for the induction of protective CTL immunity against tumors and many pathogens (3). The specialized capacity of mouse CD8α/CD103+ DCs for CTL induction is due to their superior ability to internalize cellular Ag (such as necrotic tumors or virally infected cells), process it, and present it for recognition by CTLs, a process known as cross-presentation (5). Human CD141+ DCs share this ability to cross-present cellular Ags to CTLs (6–9). Both human CD141+ DCs and mouse CD8α/CD103+ DCs also express high levels of TLR 3, an enhancer of cross-presentation (10), and the chemokine receptor XCR1, whose ligand XCL1 is secreted by activated T cells and is required for optimal CTL generation (11). The specialized capacity of these DCs for cross-

presentation is further mediated by their unique expression of the C-type lectin-like receptor (CLR) CLEC9A (also termed DNGR1) (12–14). CLEC9A recognizes dead cells, specifically F-actin exposed on the surface of dead cells, and delivers dead cell–associated Ag to the early and recycling endosomes most favorable for cross-presentation, thereby regulating cross-priming to CD8+ T cells (15–18). In mice, delivery of Ag specifically to CD8α+/CD103+ DCs in vivo induces potent CD4+ and CD8+ antiviral and antitumor immune responses (19), providing a strong rationale for the development of new vaccine strategies that specifically target their human equivalents, the CD141+ DC, in vivo. Furthermore, the presence of CD103+/CD141+ DC transcripts correlates with tumor regression and improved survival in both mouse and human cancers, supporting a pivotal role for these cells in tumor immune responses (20). Indeed, in mice, this DC subset has proved to be essential for effective CD137 or PD-1 checkpoint blockade therapy, and stimulation of these DCs with FMS-like tyrosine kinase 3 ligand (Flt3L) and poly:ICLC had a synergistic effect on antitumor responses (21). Thus, specifically targeting human CD141+ DCs is an attractive strategy for the development of new vaccines against cancer and pathogens where CTL responses are critical for immunity (1, 19, 22).

Abs that engage CLRs expressed by DCs can be used as vehicles to carry antigenic cargo directly to DCs in vivo and are emerging as attractive candidates for the design of new vaccines. Abs specific for human CLRs DCIR or DC-SIGN can deliver Ag to human in vitro–derived DCs for recognition by T cells (23, 24), and Ag targeted via the mannose receptor (MR) induced humoral and T cell responses in a human phase I clinical study (25). However, these receptors are expressed by macrophages and monocyte-derived DCs but not by CD141+ DCs (26). Abs specific for the CLR DEC-205 deliver Ag to the mouse CD8α+/CD103+DC subset in vivo to induce Ag-specific CD4+ and CD8+ T cell responses in the presence of adjuvant (27–30). Anti–DEC-205 Ab conjugated to HIV Gag Ag induces modest CD8+ T cell responses in nonhuman primates but confers no advantage compared with nontargeted protein for the induction of CD4+ T cell responses (31). Administration of anti–human DEC-205 conjugated to tumor Ag NY-ESO-1 is feasible, well tolerated, and can induce Ag-specific T cell responses in some patients with solid cancers (32). Although DEC-205 is expressed by CD141+ DCs and can deliver Ag to CD141+ DCs for cross-presentation (33), it is also expressed by other DC subsets and many other leukocytes (34), making it less suited to specifically target human CD141+ DCs and potentially reducing the Ag load available to CD141+ DCs.

The exclusive expression of CLEC9A by human CD141+ DCs combined with its role in dead-cell recognition and cross-presentation makes it a particularly attractive candidate to utilize for specifically targeting human CD141+ DCs (12–15, 18). Anti–mouse CLEC9A Abs can deliver Ags to mouse CD8α+ DCs in vivo for priming potent CTL, CD4+ T cell, and humoral responses and protective antitumor immunity (12, 13, 35–39). When compared with anti–mouse DEC-205 Ab, targeting with anti-CLEC9A Ab is at least as effective at inducing CTL responses (35, 37). However, anti-CLEC9A Ab persists longer in the bloodstream, resulting in prolonged Ag presentation and superior CD4+ T cell and humoral immune responses (35). Rat anti–human CLEC9A Ab induce humoral responses in nonhuman primates (40) and human CLEC9A can facilitate Ag presentation by CD141+ DCs to CD4+ and CD8+ T cells (26), providing a strong rationale for the development of anti–human CLEC9A Abs to deliver Ag to CD141+ DCs for immunotherapy. The focus of this study was to develop human chimeric anti-CLEC9A and anti–DEC-205 Abs and investigate the ability of human anti-CLEC9A to deliver Ag for processing and presentation to CD4+ and CD8+ T cells.

Results

Generation of human chimeric Ab targeting CLEC9A and DEC-205. Human chimeric Abs specific for CLEC9A, DEC-205, and β-gal (nontargeting isotype control) were generated, containing the variable regions of rat anti–human CLEC9A (12), rat anti–β-gal GL117 mAb (35, 41), or mouse anti–human DEC-205 mAb (34), with human IgG4 and κ constant regions. A 40-aa fragment of CMVpp65 containing both CD4+ and CD8+ T cell epitopes was selected as a proof-of-principle Ag and also as a promising vaccine target for the prevention of CMV disease (42). A FLAG tag was included at the C-terminus of the CMVpp65 Ag to facilitate Ag detection. The CMVpp65 Ag and a FLAG tag were genetically fused to the C-terminus of the Ab heavy chain to generate recombinant Ab-pp65 (Figure 1A). Both purified anti-CLEC9A and anti–DEC-205 Ab-pp65 maintained their ability to bind their respective targets expressed on the cell surface of transfected cell lines (Supplemental Figure 1A; supplemental material available online with this article; doi:10.1172/jci.insight.87102DS1). All the Ab-pp65 bound their target protein or peptides by ELISA; effective binding was detected using both anti–human IgG4 and anti-FLAG Ab, confirming the presence of the pp65 Ag
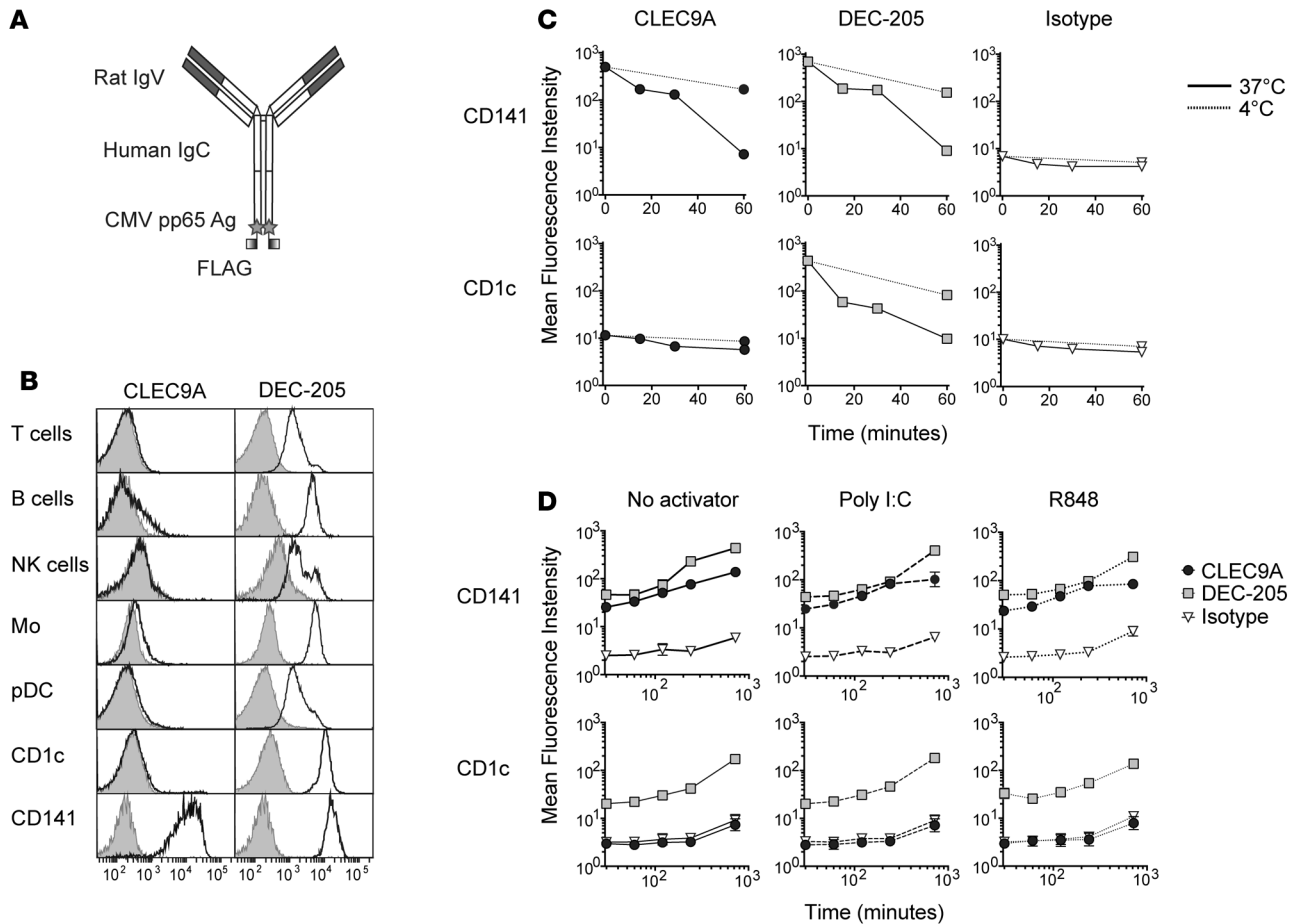
Figure 1. Generation, internalization, and accumulation of human chimeric Ab-pp65 fusion proteins. (**A**) Diagram of human chimeric mAb, consisting of rat or mouse variable regions joined to human IgG4 and κ constant regions, genetically fused to the CMV pp65 antigen (Ag) and FLAG tag via linker sequences. (**B**) Binding of human chimeric Ab to human PBMCs was assessed by incubating PBMCs with anti-CLEC9A Ab (black, left panel), anti–DEC-205 Ab (black, right panel), or isotype Ab (gray), detected with anti–human IgG4-biotin and streptavidin-PE and analyzed by flow cytometry. Data are representative of 2 independent experiments. (**C**) DCs were incubated with human chimeric Ab at 4°C for 30 minutes and subsequently incubated at 4°C or 37°C. DCs were stained with anti–human IgG-biotin and streptavidin-PE at indicated time points to label remaining surface-bound Ab and analyzed by flow cytometry. Data shown are the mean fluorescence intensity (MFI) and are representative of 3 independent experiments from different donors. (**D**) Accumulation of human chimeric Ab by human DCs enriched from PBMCs. Alexa Fluor 488–labeled (AF 488–labeled) human chimeric Abs were cultured with DCs at 37°C for up to 12 hours in the presence or absence of poly I:C or R848. Cells were counterstained for HLA-DR, live/dead aqua, CD141, and CD1c and analyzed by flow cytometry. Data show the MFI, which was normalized for conjugation efficiency of the human chimeric Ab, and are the mean ± SD of 3 donors.

(Supplemental Figure 1B). The anti-CLEC9A Ab bound solely to the CD141⁺ DC subset (Figure 1B), consistent with the original rat mAb (12). By contrast, the anti–DEC-205 Ab bound to all human leukocyte subsets, consistent with the original mouse mAb (34), with the highest expression on CD1c⁺ and CD141⁺ DCs, whereas the isotype control did not demonstrate any binding (Figure 1B). Both anti-CLEC9A and anti–DEC-205 Abs stained CD141⁺ DCs with similar intensity.

Human chimeric Abs are internalized and accumulate within cDCs. The internalization of human chimeric Abs by CD141⁺ and CD1c⁺ DCs was investigated by coating cells with saturating amounts of Ab, prior to culture at 37°C or 4°C, and then detecting the Ab remaining on the cell surface using anti–human IgG4 secondary Ab (Figure 1C). Anti–DEC-205 and anti-CLEC9A Ab bound to the surface of CD141⁺ DCs decreased at a similar rate during culture at 37°C and were undetectable after 1 hour. Anti–DEC-205, but not anti-CLEC9A or isotype control Ab, bound to CD1c⁺ DCs and detectable levels of the Ab diminished over 1 hour of culture at 37°C. To determine whether the diminished cell surface staining was the result of internalization or dissociation of the Abs from their surface receptor, the accumulation of Alexa Fluor (AF) 488–labeled human chimeric Ab by DCs was investigated (Figure 1D). The fluorescence intensity of anti-CLEC9A and anti–DEC-205 Abs on CD141⁺ DCs increased over time, suggesting that loss of surface staining observed in Figure 1C was the result of Ab internalization and subsequent accumulation
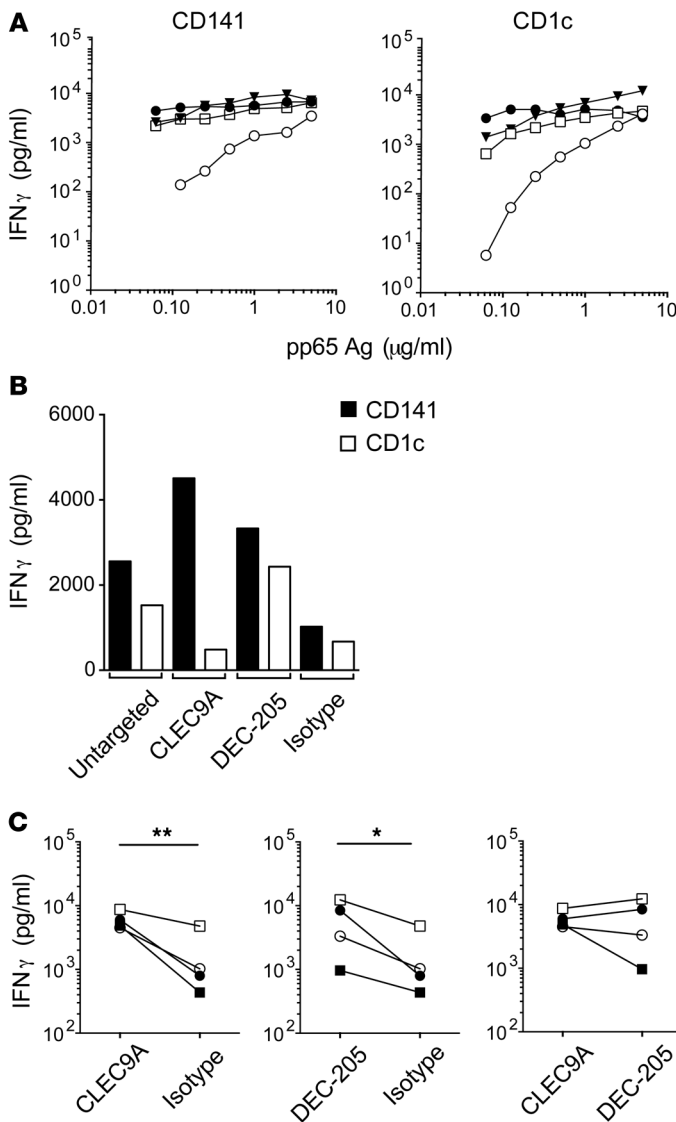
Figure 2. Presentation of pp65 antigen by blood DCs in vitro to CD4+ T cells. CD1c+ and CD141+ DCs were isolated from PBMCs and cultured with antigen (Ag) for 2 hours at 37°C. DCs were washed and cultured overnight with AGILARNLVPMVATV-specific (AGI-specific) CD4+ T cells. IFNγ production was measured by ELISA. (**A**) DCs were cultured with titrated concentrations of the soluble pp65 Ag. Data are shown as mean concentrations of technical replicates, and each symbol represents one of 4 donors. (**B**) Isolated CD1c+ (white) and CD141+ (black) DCs were cultured with 0.25 μg human chimeric Ab-pp65 fusion proteins or the equivalent concentration of soluble untargeted Ag. The background level of IFNγ was subtracted. Data are shown as mean concentration of technical replicates and are representative of 4 donors. (**C**) Ag presentation following targeting with Ab-pp65 fusion proteins by CD141+ DCs in 4 donors. Background level of IFNγ was subtracted. Each symbol represents the mean concentration of technical replicates from an independent donor. *$P < 0.05$, **$P < 0.01$; 2-tailed ratio-paired Student's t test.

within the cell. The anti–DEC-205 Ab also accumulated in CD1c+ DCs over time, while the isotype control Ab did not markedly accumulate in either subset (Figure 1D). Activation of the DCs with either polyI:C or R848 did not affect the rate of Ab accumulation within the cell (Figure 1D). These results demonstrate that the human chimeric anti-CLEC9A Ab and anti–DEC-205 Ab internalized and accumulated within CD141+ DCs at a similar rate in vitro.

Ag presentation to CD4+ T cells in vitro. We initially assessed the ability of both CD141+ and CD1c+ DCs to present the pp65 Ag to HLA-DR3–restricted AGILARNLVPMVATV-specific (AGI-specific) CD4+ T cell lines. We confirmed that soluble pp65 Ag could be equally processed and that the AGI epitope was presented by HLA–DR3-restricted CD141+ DCs and CD1c+ DCs (Figure 2A). Both anti–CLEC9A-pp65 and anti–DEC-205-pp65 delivered Ag for presentation of the AGI epitope in vitro, with anti–CLEC9A-pp65 effectively targeting CD141+ DCs and anti–DEC-205-pp65 delivering Ag to both CD141+ and CD1c+ DCs (Figure 2B). When multiple donors were compared, delivery via CLEC9A and DEC-205 was similar and significantly more effective than the isotype control (Figure 2C). Thus, targeting with human chimeric anti-CLEC9A and anti–DEC-205 Abs can efficiently deliver Ag for processing and presentation to CD4+ T cells in vitro.

Cross-presentation by blood CD141+ and CD1c+ DCs to CD8+ T cells in vitro. The ability of CD141+ and CD1c+ DCs to cross-present the pp65 Ag to HLA-A*0201–restricted NLVPMVATV-specific (NLV-specific) CD8+ T cell lines was assessed. In 2 of 3 donors examined, CD141+ and CD1c+ DCs displayed similar capacity to cross-present the soluble pp65 Ag, although in 1 donor, CD1c+ DCs were more efficient at lower Ag concentrations (Figure 3A). Targeting Ag via CLEC9A resulted in substantially enhanced cross-presentation by CD141+ DCs when compared with the isotype control, anti–DEC-205-pp65, and an equivalent amount of untargeted soluble pp65 Ag (Figure 3B). The efficacy of anti–CLEC9A-pp65 compared with the isotype control and DEC-205-pp65 was evident when multiple donors were examined. CLEC9A targeting was significantly more effective than the isotype control or DEC-205 targeting for all donors (Figure 3C). The addition of poly I:C resulted in non–Ag-specific activation of T cells in all conditions and did not enhance cross-presentation following targeting with anti–CLEC9A-pp65 (Figure 3D). Overall, these data demonstrate that the human chimeric anti-CLEC9A Ab efficiently delivers Ag specifically to CD141+ DCs for cross-presentation to CD8+ T cells and is more effective compared with DEC-205–targeted and nontargeted delivery.
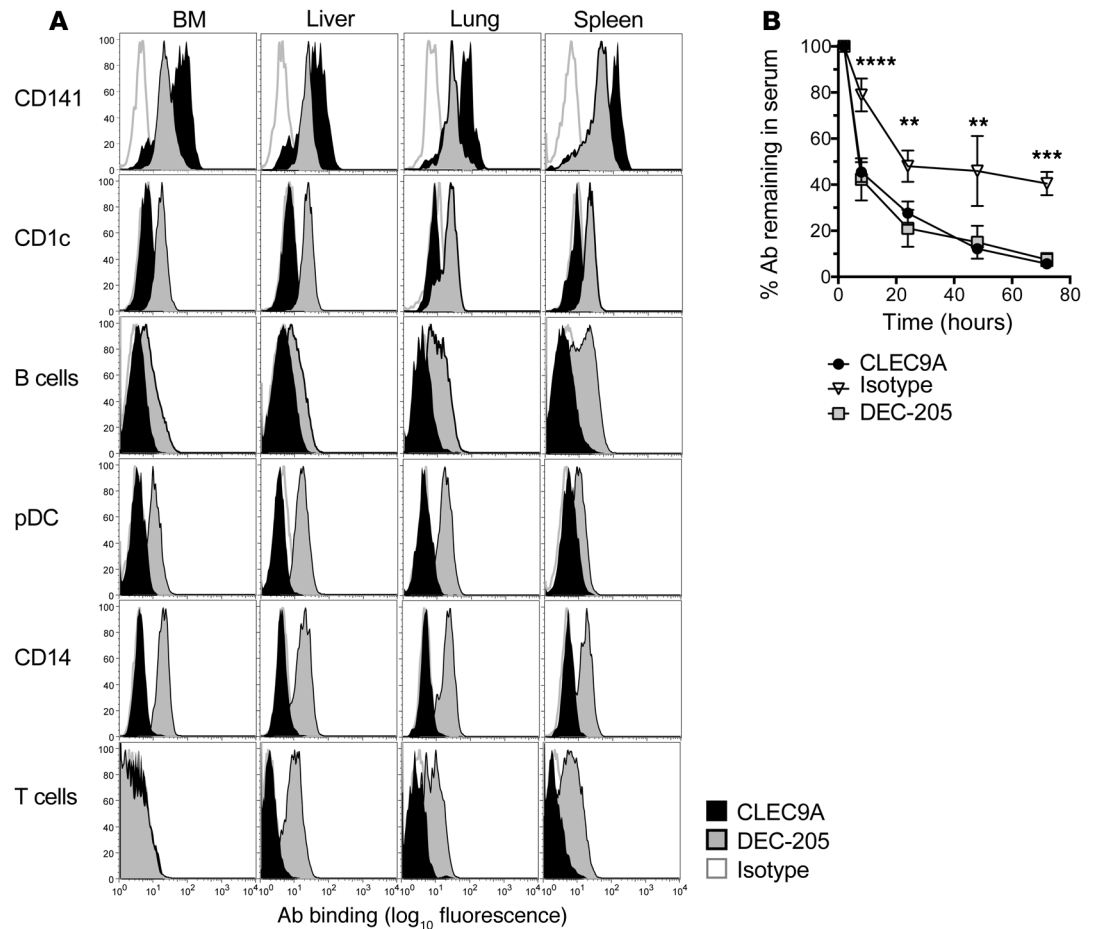
Targeting of human DCs in humanized NSG-A2 mice. We next investigated whether anti-CLEC9A Ab could effectively target human CD141+ DCs in vivo. We utilized a humanized NSG-A2 (huNSG-A2)
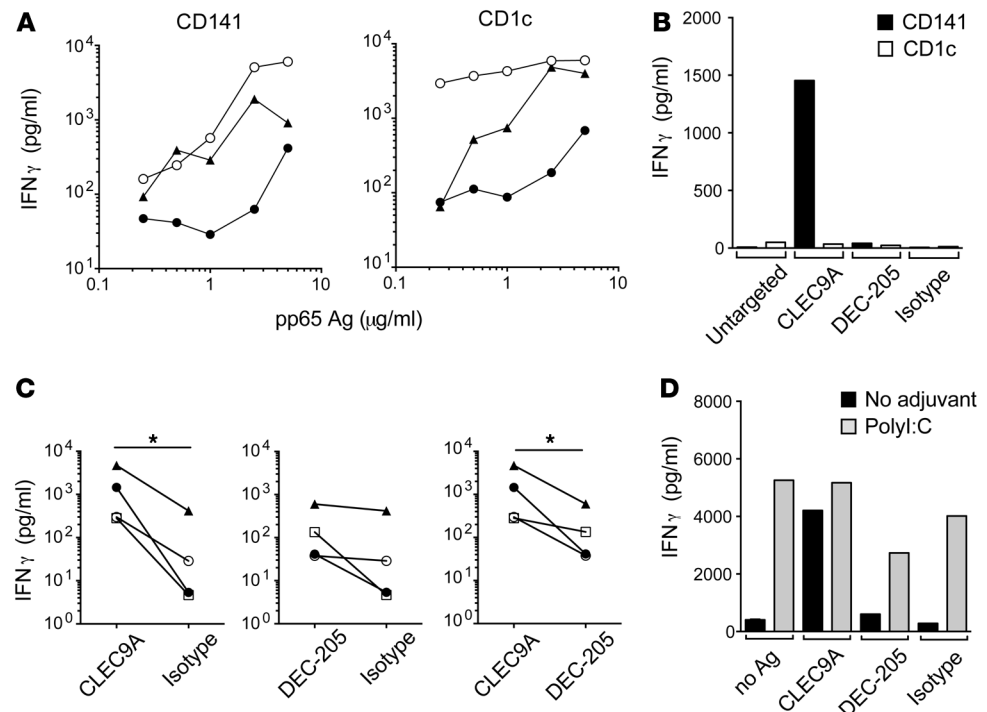
Figure 3. Cross-presentation of pp65 antigen by blood DCs in vitro. CD1c⁺ and CD141⁺ DCs were isolated from PBMCs and cultured with antigen (Ag) for 2 hours at 37°C. DCs were washed and cultured overnight with NLVPMVATV-specific (NLV-specific) CD8⁺ T cells. IFNγ production was measured by ELISA. (**A**) DCs were cultured with titrated concentrations of the soluble pp65 Ag. Data are the mean concentration of technical replicates, and each symbol represents one of 3 donors. (**B**) Isolated CD1c⁺ (white) and CD141⁺ (black) DCs were cultured with 1 μg human chimeric Ab-pp65 fusion protein or the equivalent concentration of untargeted Ag. Data are shown as mean concentration of technical replicates and are representative of 3 donors. (**C**) Cross-presentation following targeting with Ab-pp65 fusion protein by CD141⁺ DCs in 4 donors. Each symbol represents the mean concentration from an independent donor. *$P < 0.05$, 2-tailed ratio paired Student's t test. (**D**) Cross-presentation by CD141⁺ DCs in the presence (gray) and absence (black) of 25 μg/ml polyI:C as in **B**. Data are shown as mean concentration of technical replicates and are representative of 2 donors.

mouse model reconstituted with human CD34⁺ cord blood cells to enable development of functional human T and B cells, monocytes, plasmacytoid DCs (pDCs), and conventional DCs (cDCs) in vivo (43). Injected AF-488–conjugated anti-CLEC9A Ab specifically bound to CD141⁺ DCs in both lymphoid and nonlymphoid tissues, while the anti–DEC-205 Ab bound to CD141⁺ DCs and to all other cell types examined. In contrast, the isotype control did not bind at all (Figure 4A). The efficacy of targeting Clec9A in the mouse has been shown to be partly due to its prolonged persistence in serum when compared with DEC-205 or other receptors (35). Therefore, we evaluated the persistence of the human chimeric Ab within the huNSG-A2 mouse over time. The isotype control showed significantly higher persistence 8 hours to 3 days after injection, while anti-CLEC9A and anti–DEC-205 Abs decreased more rapidly but were comparable and still detectable at 3 days (Figure 4B).

We subsequently investigated Ag delivery and cross-presentation via anti–CLEC9A-pp65 in vivo. These experiments were conducted in the presence of poly I:C, as no cross-presentation was detected in the absence of activation in this model (K.M. Tullett, M.H. Lahoud, and K.J. Radford, unpublished observations). Targeted Ab-pp65 fusion proteins persisted in the serum in the presence of poly I:C, similarly to the original chimeric Ab (Figure 5A). Anti–CLEC9A-pp65 and anti–DEC-205-pp65 delivered Ag to CD141⁺ DCs for cross-presentation more effectively than the isotype control across all cohorts of mice (Figure 5B). However, CD1c⁺ DCs were only able to cross-present DEC-205–targeted Ag in 2 of 6 independent experiments, each using huNSG-A2 mice engrafted from a different cord blood donor (Figure 5B). Where feasible, multiple mice were engrafted with the same cord blood and Ab-pp65 was directly compared within the same cohort (termed paired mice) to minimize any variation observed between different donors (Figure 5, C and D). Consistent with the unpaired data in Figure 5B, targeting via CLEC9A on CD141⁺ DCs was significantly more efficacious than the isotype control (Figure 5C). Targeting of DEC-205 on CD141⁺ DCs
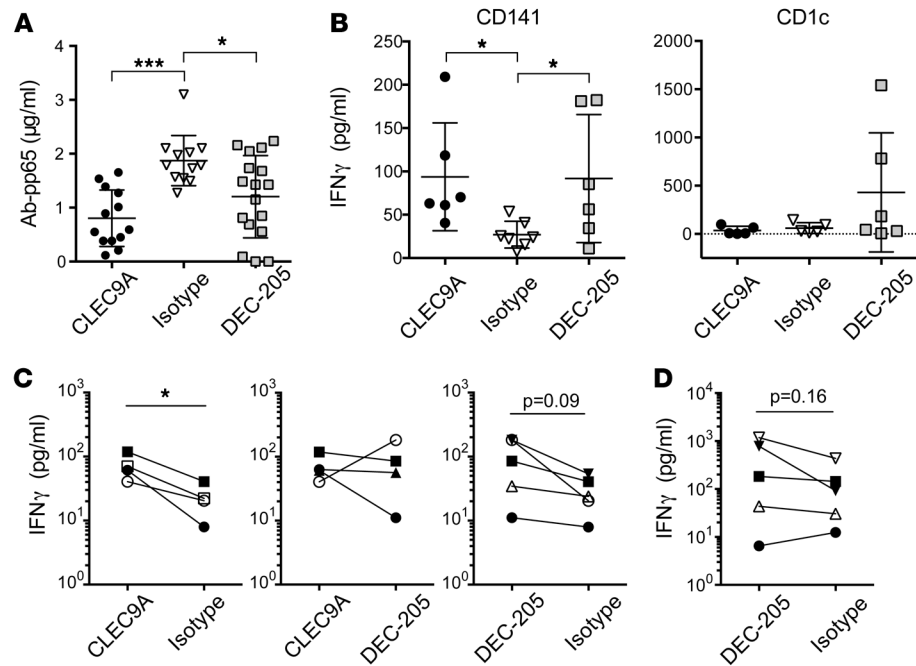
Figure 4. Targeting of human DCs in vivo with human chimeric Ab in huNSG-A2 mice. (A) Binding of Alexa Fluor 488–labeled (AF 488-labeled) human chimeric Ab to human lymphocyte subsets following i.v. injection into huNSG-A2 mice; representative of 3 experiments. **(B)** Serum concentrations of human chimeric Ab in huNSG-A2 mice as measured by ELISA at indicated time points. Data are shown as a mean percentage ± SD of 3 independent experiments. **$P < 0.01$ (24 and 48 hours; isotype vs. CLEC9A and DEC-205), ***$P < 0.001$ (72 hours; isotype vs. CLEC9A and DEC-205), ****$P < 0.0001$ (8 hours; isotype vs. CLEC9A and DEC-205), 2-way ANOVA, Tukey's multiple comparisons test.

was also appreciably more effective than the isotype control, although this was not significant in paired mice (Figure 5C), nor was DEC-205 targeting to CD1c$^+$ DCs (Figure 5D). Both anti-CLEC9A and anti–DEC-205 Abs targeted human CD141$^+$ DCs in the presence of polyI:C in our humanized mouse model. In conclusion, targeting CD141$^+$ DCs using CLEC9A is highly effective for inducing both CD4$^+$ and CD8$^+$ T cell responses and can demonstrate more effective responses than DEC-205 targeting under certain conditions, providing a strong rationale for pursuing anti-CLEC9A Ab for immunotherapy.

Discussion

This study reports the development of a chimeric human IgG4 Ab specific for human CLEC9A that specifically binds to, is internalized by, and accumulates within human CD141$^+$ DCs, enabling effective Ag presentation. Our chimeric Abs were constructed using human IgG4 κ modified to contain point mutations to stabilize disulfide bonds and minimize nonspecific FcR binding (24, 44, 45), and they were genetically fused with 2 Ag molecules to allow direct comparisons between CLEC9A and DEC-205. Ab-pp65 fusion proteins delivered Ag for processing and presentation to both CD4$^+$ and CD8$^+$ T cells in vitro. In huNSG-A2 mice comprising functional human DC subsets, we demonstrated that human chimeric anti-CLEC9A Ab is specifically taken up by CD141$^+$ DCs in lymphoid and nonlymphoid tissues in vivo, including BM, spleen, liver, and lung. We further demonstrated that CLEC9A-targeted Ag was efficiently delivered to the cross-presentation pathway in CD141$^+$ DCs in vivo. Targeting human CD141$^+$ DCs using

Figure 5. Targeting of human DCs in vivo with Ab-pp65 fusion protein and ex vivo cross-presentation. (A) Serum concentrations of Ab-pp65 in huNSG-A2 mice 24 hours after i.v. injection with Ab-pp65 and poly I:C. Each point represents mean concentration from 1 mouse (CLEC9A, *n* = 13; DEC-205, *n* = 17; Isotype, *n* = 12). Bars are mean ± SD. *P < 0.05, ***P < 0.001, 2-way ANOVA, Tukey's multiple comparisons test. **(B)** Cross-presentation by huNSG-A2 splenic CD141+ and CD1c+ DCs 24 hours after i.v. injection with Ab-pp65 and poly I:C. DCs were cultured ex vivo with NLVPMVATV-specific (NLV-specific) CD8+ T cells, and IFNγ production was measured by ELISA. Each point represents the mean concentration of technical replicates from an individual experiment with independent cord-blood donors (CLEC9A and DEC-205, *n* = 6; isotype, *n* = 7). Bars are mean ± SD, *P < 0.05, 2-tailed paired Student's *t* test. **(C)** Ex vivo cross-presentation by CD141+ to NLV-specific CD8+ T cells. Each point represents the mean concentration of technical replicates from individual cord-blood donors and independent experiments, represented by different symbols (CLEC9A, *n* = 4; DEC-205, *n* = 5), *P < 0.05, 2-tailed paired Student's *t* test. **(D)** Ex vivo cross-presentation by CD1c+ to NLV-specific CD8+ T cells. Each point represents the mean concentration of technical replicates from an individual cord-blood donor and independent experiment; *n* = 5. Data were analyzed by paired Student's *t* test.

human chimeric anti-CLEC9A Ab is therefore an attractive strategy as a therapeutic vaccine for disease settings such as cancer and many viruses where CTL responses are considered essential.

When directly compared with anti–DEC-205 Ab, anti-CLEC9A Abs bound to CD141+ DCs with similar intensity and were internalized and accumulated within these cells at a similar rate. We demonstrated that anti-CLEC9A Abs were more efficient at delivering Ag for presentation to both CD4+ and CD8+ T cells compared with the equivalent concentrations of soluble Ag or Ag delivered by the isotype control Ab in vitro. While anti–DEC-205-pp65 efficiently delivered Ag to both CD141+ DCs and CD1c+ DCs for processing and presentation to CD4+ T cells, it was ineffective at delivering the Ag to the cross-presentation pathway of either DC subset for recognition by CD8+ T cells in vitro. This contrasts with some previous reports of cross-presentation via anti–DEC-205-Ag fusion proteins in vitro (46–48). In these studies, cross-presentation of multiple epitopes within the fusion protein was detected by polyclonal T cell lines, which are likely more sensitive than assays detecting single epitopes. These studies also fused full-length Ag (144- to 241-aa long) to DEC-205 Ab, which may be less resistant to degradation (49), thereby allowing greater access of Ag to the cross-presentation pathway compared with shorter Ags as used in our study. Cohn et al. (33) showed that short peptide Ag chemically conjugated to DEC-205 Ab could be delivered for cross-presentation by CD141+ DCs but not CD1c+ DCs. Differences in degradation kinetics of the Ag, chimeric Ab fusion, and sensitivity of the responding T cells may account for why we were unable to detect cross-presentation following targeting with anti–DEC-205 Ab to CD141+ DCs in vitro. Regardless, we found that targeting with anti-CLEC9A Ab was significantly more effective at cross-presentation compared with anti–DEC-205 Ab in vitro. This is consistent with their intracellular localization after internalization. Whereas DEC-205 traffics to late endosomes and lysosomes typically associated with MHC II Ag presen-

tation, CLEC9A traffics to early endosomes that are more favorable for cross-presentation (17, 33, 49–51). Our findings that DEC-205 and CLEC9A Abs are equivalent at delivering Ag for recognition by CD4+ T cells concurs with other data showing efficient MHC II processing from early endosomes (33), eliminating any advantage conferred through delivery to late endosomes with DEC-205.

In contrast to the in vitro assays, both anti-CLEC9A and anti–DEC-205 Abs delivered Ag to CD141+ DCs for cross-presentation in vivo. The reasons for the discrepancy between the in vitro and in vivo data are not clear, but as cross-presentation by anti–DEC-205 Ab only occurs with high Ab concentrations in vitro (33), differences in vivo may become more apparent at more limiting Ab doses. However, our in vivo data in the huNSG-A2 model are consistent with mouse models where CLEC9A and DEC-205 Abs are comparable at inducing CD8+ T cell responses (35, 37). Low-level cross-presentation by DEC-205 (below the detection limits of our assay) may be compensated for in vivo by the ability of DEC-205 to target a larger number of DCs, including CD1c+ DCs and pDCs. It is also possible that cooperation by different DC subsets and, in particular, bystander effects of cytokines may influence cross-presentation in vivo but would not be apparent in vitro. There may be some instances where the broader specificity of DEC-205 could be advantageous, enabling targeted Ag to be delivered to all DC types and facilitating DC cooperation for the induction of immunity or tolerance. In particular, targeting via DEC-205, in the absence of adjuvants, is likely to offer advantages for the induction of tolerance (52). Indeed, mouse models have demonstrated its efficacy in the treatment of allergy and autoimmune arthritis (53, 54).

In mice, anti-CLEC9A Ab persists longer than anti–DEC-205 Ab (35), whereas in our huNSG-A2 model, both Abs were eliminated from the serum at a similar rate. This disparity probably reflects a number of factors: in the classical mouse model, DEC-205 is expressed on DC subsets, and on leukocytes and gut, thymus, and lung endothelia; stromal BM; and brain tissue capillaries (55, 56); thus, anti–DEC-205 Ab can be more readily absorbed from the serum. In contrast, in huNSG-A2 mice, human DEC-205 is expressed on DCs and all leukocytes, but other tissues (e.g., gut, endothelia, brain tissue capillaries) are of mouse origin and therefore do not express human DEC-205. Thus, anti–human DEC-205 Abs can persist for longer in this model. In humans, we would predict that the broad expression pattern of DEC-205 would result in reduced anti–DEC-205 Ab-Ag persistence, while anti-CLEC9A Ab-Ag persistence would be prolonged due to the selective specificity of CLEC9A, thereby potentiating immune responses.

The requirement for activation for cross-presentation by human DCs in vitro is currently unclear and appears to vary depending on the size and nature of the Ag and the source of the DC. Previous studies targeting human DCs in vitro have reported cross-presentation to T cells, either in the absence (46) or presence of activators (26, 33, 48, 49), but did not directly compare both conditions. Our direct comparisons revealed that, in vitro, CLEC9A-mediated cross-presentation by CD141+ DCs did not require activation; furthermore, the addition of polyI:C did not enhance cross-presentation. In contrast, in vivo, we only observed cross-presentation in the presence of activation. We anticipate that, in vivo, human cross-priming for CTL induction will require activation, consistent with mouse in vivo targeting studies that require activation for cross-priming (12, 35, 37).

Although a number of strategies are currently being investigated for targeting of human DCs in vivo, our study is the first to our knowledge to report an Ab construct that specifically targets the human CD141+ DC subset in vitro and in vivo and delivers Ag for recognition by CD4+ and CD8+ T cells. Like CLEC9A, the chemokine receptor XCR1 is exclusively expressed by CD141+ DCs. The XCR1 ligand, XCL1, and XCR1 Ab have been used to deliver Ag to mouse CD8α+ DCs (57, 58). Whether human CD141+ DCs can be specifically targeted via XCR1 and how this compares to CLEC9A targeting is worthy of investigation.

In this study, we focused on developing human chimeric anti-CLEC9A Ab for the delivery of a viral CMV Ag, as proof of principle. Our constructs have been designed to enable expression of anti-CLEC9A Ab with different antigenic cargo, such as pathogen- or tumor-associated Ag, facilitating the application of this platform to different vaccines and immunotherapies. While some clinically used Abs are fully humanized (46), others are human chimeric Abs either containing whole variable regions or complementarity determining regions from the host species (59). Our current constructs contain rat variable regions with human constant regions. Immunogenicity studies will determine whether the nonhuman regions of our targeting Ab initiate an unwanted immune response and warrant further humanization (60).

We anticipate that, for cancer immunotherapy, CLEC9A targeting would be particularly effective in combination with strategies for overcoming the suppressive tumor environment. Abs against immune regulators of T cell function such as CTLA-4, PD-1, and CD137 (42, 61, 62) are likely to combine well with targeting CD141+ DCs, as the cross-presenting DC lineage has been shown to be important for effective

checkpoint blockade therapy in mouse models (21). CLEC9A plays a critical role in Ag recognition and regulation of cross-priming (17), and targeting CLEC9A has shown great promise in mouse and primate models (13, 35, 40). Our research extends these studies, demonstrating that human chimeric anti-CLEC9A Abs specifically and efficiently deliver Ag to human CD141^{+} DCs, in vitro and in vivo, for recognition by CD4^{+} and CD8^{+} T cells. This provides strong support for the use of CLEC9A as a potential target for exploiting CD141^{+} DCs in immunotherapy.

Methods

Study design. The objective of this study was to develop human chimeric Abs to CLEC9A, DEC-205, and an isotype control for Ag delivery to human DCs. In vitro studies targeting human DCs used blood or apheresis product obtained from healthy donors: 3 donors for internalization and accumulation studies and 4 donors for Ag presentation studies.

In vivo studies utilized huNSG-A2 mice engrafted with human cord blood CD34^{+} cells, with the number of mice indicated above. In vivo targeting with human chimeric Ab was assessed in 3 huNSG-A2 mice per time point. Ab-pp65 persistence in the presence of polyI:C was examined in 12–14 huNSG-A2 mice engrafted from 6–7 independent cord blood donations (Figure 5A). In vivo targeting with each Ab-pp65 was assessed in 6–7 huNSG-A2 mice, each engrafted with an individual cord-blood donation (Figure 5B). Where possible, a cohort of mice was engrafted with a single cord-blood donation, and targeting with each Ab was directly compared within each cohort of mice, eliminating donor-to-donor variation and allowing paired analysis of the data (Figure 5, C and D).

Time points for internalization, accumulation, and Ab persistence assays were selected based on pilot experiments and previous studies (12, 33, 35). All data points were included in analyses, and outliers were not excluded.

Generation of human chimeric Ab-Ag fusion constructs. The cDNAs encoding Ab chains were amplified from hybridomas: anti-CLEC9A, clone 23/05-4C6 (12); anti–DEC-205, clone MMRI-7 (34); and anti–β-gal rat IgG2a isotype control, clone GL117 (35, 41) as described previously (35). Hybridomas were generated in house at Mater Research Institute or The Walter and Eliza Hall Institute of Medical Research. Plasmids encoding heavy and light chains in pcDNA3.1[+] were generated by gene synthesis of codon-optimized variable region sequences in frame with either the human IgG4 constant region sequence or human κ constant region (GeneArt) (24). Two point mutations were introduced to the human IgG4 constant region (S229P and L236E) to stabilize disulfide bonds and abrogate FcR binding (24). The heavy chain was fused to antigenic sequence (AAAKNMIIKPGKISHIMLDVAPPWQAGILARNLVPMVATVQGQSGSGDY-KDDDDK) containing the CMV pp65 HLA-DR3–restricted epitope AGI and HLA-A*0201–restricted epitope NLV and a FLAG tag DYKDDDDK to facilitate purification and detection of Ab-pp65. Thus, recombinant Ab-pp65 carried 2 Ags per Ab molecule. Ab-pp65 was expressed in mycoplasma-free Freestyle 293F cells (Invitrogen) using 293Fectin (Invitrogen) and purified from the culture supernatant by affinity chromatography using anti-FLAG M2-agarose beads (Sigma-Aldrich), followed by size-exclusion chromatography using Superdex 200 or Superose 6 columns (GE Healthcare).

Validation and detection of human chimeric Ab. The integrity of the human chimeric Ab and Ab-pp65 was validated by binding to 293F cells transiently transfected with full-length recombinant CLEC9A or DEC-205 (12, 63). Bound Ab was detected using anti–human IgG4-biotin (Invitrogen, catalog A10663) and streptavidin-PE (BD Pharmingen, catalog 554061) by flow cytometry. The Ab-pp65 was further validated by assessing its capacity to bind peptides or recombinant proteins by ELISA. Bound Abs were detected with anti–human IgG4-biotin and Streptavidin-HRP (GE Healthcare, catalog RPN4401) or M2-HRP (anti-FLAG-HRP) (Sigma-Aldrich) and visualized with ABTS.

Isolation of human DCs. PBMCs were isolated from whole blood or leukapheresis product using Ficoll-Paque Plus density gradient centrifugation (GE Healthcare). DCs were enriched using the Myeloid DC enrichment kit (Stemcell Technologies) and stained with Abs: CD3 (clone OKT3-Pacific Blue), CD14 (clone HCD14-Pacific Blue), CD16 (clone 368-Pacific Blue), CD19 (clone HIB19-Pacific Blue), CD20 (clone 2H7-Pacific Blue), CD56 (clone B159-Pacific Blue), CD1c (clone L161-PE), CD141 (clone M80-APC), HLA-DR (clone L243-PE-Cy7), and live/dead aqua (all from BioLegend). For Ag presentation assays, DC subsets were sorted on a MoFlo Astrios (Beckman Coulter), routinely yielding >95% purity (Supplemental Figure 2). Cells were maintained in complete medium (RPMI 1640 supplemented with GlutaMAX, 10% AB serum, 100 U/ml penicillin, 100 μg/ml streptomycin, 1 mM sodium pyruvate,

0.1 mM nonessential amino acids, 10 mM HEPES, and 50 μM 2-ME) at 37°C and 5% CO_2.

Ab internalization and accumulation assays. Enriched DCs were incubated with human chimeric Ab at 4°C for 30 minutes, washed, and incubated for indicated times at 4°C or 37°C in complete AB medium. Cell surface Ab was detected with anti–human IgG4-biotin and streptavidin-PE by flow cytometry on a CyAn ADP analyzer (Beckman Coulter) and analyzed with FlowJo (Tree Star Inc.). To measure accumulation of the human chimeric Ab within the DCs, Abs were AF-488 conjugated (Invitrogen) and incubated with enriched cDCs in complete media at 37°C for indicated time periods, followed by flow cytometric analysis.

Ag presentation to CD8^{+} and CD4^{+} T cells. DCs from HLA-A*0201^{+} or HLA-DR3^{+} donors were incubated for 2 hours in the presence of Ab-pp65 proteins or pp65 Ag (GL Biochem) in the presence or absence of 25 μg/ml polyI:C (InvivoGen). DCs were washed and cultured overnight with NLV-specific CD8^{+} T cells (DC/T cell ratio 1:3) or AGI-specific CD4^{+} T cells (DC/T cell ratio 1:5). IFNγ production by T cells was detected in the supernatants by ELISA (eBioscience).

Generation and immunization of huNSG-A2 mice. NSG-A2 mice (NOD.Cg-Prkdcscid Il2rgtm1Wjl Tg[HLA-A2.1]1Enge/SzJ) were purchased from The Jackson Laboratory and a breeding colony established in-house. CD34^{+} progenitors were isolated from cord-blood donations using a CD34^{+} isolation kit (Miltenyi Biotec). huNSG-A2 mice were generated as previously described (43) with minor modifications. Female NSG-A2 mice (10–12 weeks old) were sublethally irradiated (250 cGy) and transplanted i.v. 24 hours later with 2×10^5 CD34^{+} cells. Engraftment was confirmed at 4 weeks by detection of huCD45^{+} cells in blood. Engrafted mice were injected s.c. with 50 μg Flt3L-Ig (BioXCell) at 1 and 4 days before harvesting cells at 9 days. Engrafted huNSG-A2 mice were injected i.v. with 5 μg of human chimeric Ab for Ab persistence assays, 5 μg of human chimeric Ab AF-488 for in vivo targeting assays, and 10 μg of Ab-pp65 fusion protein and 50 μg poly I:C for ex vivo cross-presentation assays.

Purification of leukocytes from engrafted huNSG-A2 mice. Leukocytes from BM, liver, lung, and spleen were isolated as previously described (43, 64). Cells were stained with Ab as for DC isolation from peripheral blood mononuclear cells (PBMCs) with the addition of CD1c (clone B-B5-FITC) (Abcam), CD123 (clone 9F5-PE) (BD Biosciences), or huCD45 (clone H130-APC-Cy7), mouse CD45 (clone 30-F11-PerCp Cy5.5), or CD14 (clone HCD14-APC) (all from BioLegend). Human DCs were analyzed by flow cytometry or sorted using gating strategies shown in Supplemental Figures 3 and 4. For cross-presentation assays, sorted DCs were cultured with NLV-specific T cells as described above (DC/T cell ratio 10:3).

Statistics. Ag presentation assays using blood DCs were analyzed using a 2-tailed ratio paired Student's *t* test from 4 independent donors. Ab persistence over time was analyzed by 2-way ANOVA and Tukey's multiple comparisons test from 3 independent experiments. Ab-pp65 concentration at 24 hours was analyzed by one-way ANOVA and Tukey's multiple comparisons test in 12–17 mice from 6 independent experiments. Unpaired ex vivo cross-presentation by CD141^{+} and CD1c^{+} DCs was analyzed by one-way ANOVA and Tukey's multiple comparisons test for 6 independent cohorts of mice. The paired ex vivo cross-presentation data were analyzed by 2-tailed ratio paired Student's *t* test for 4–5 paired cohorts of mice. For all statistical analyses, $P < 0.05$ was considered significant.

Study approval. Cord blood was obtained from the Queensland Cord Blood Bank, and whole blood or leukapheresis products from healthy volunteers were obtained after informed consent and ethics approval from the Mater Health Services Human Research Ethics Committee (HREC 1586M and 1407AP). Mice were housed and treated in accordance with approval by the University of Queensland Animal Ethics committee (protocol 324-13).

Author contributions

KMT, MHL, and KJR designed, performed, and analyzed the research and wrote the paper. IMLR, YM, PST, CS, and JGZ performed the research and analysis. KS, IC, and RK contributed reagents, designed the research, interpreted the data, and reviewed the manuscript.

Acknowledgments

Address correspondence to: Mireille H. Lahoud, Monash University, Building 75, 15 Innovation Walk, Wellington Road, Clayton, Victoria 3800, Australia. Phone: 61.3.9905.3788; E-mail: mireille.lahoud@monash.edu. Or to: Kristen J. Radford, Mater Research, Translational Research Institute, 37 Kent St Woolloongabba, Queensland, 4102, Australia. Phone: 617.3443.7638; E-mail: kristen.radford@mater.uq.edu.au.

1. Radford KJ, Tullett KM, Lahoud MH. Dendritic cells and cancer immunotherapy. *Curr Opin Immunol*. 2014;27:26–32.
2. Guilliams M, et al. Dendritic cells, monocytes and macrophages: a unified nomenclature based on ontogeny. *Nat Rev Immunol*. 2014;14(8):571–578.
3. Merad M, Sathe P, Helft J, Miller J, Mortha A. The dendritic cell lineage: ontogeny and function of dendritic cells and their subsets in the steady state and the inflamed setting. *Annu Rev Immunol*. 2013;31:563–604.
4. Schlitzer A, Ginhoux F. Organization of the mouse and human DC network. *Curr Opin Immunol*. 2014;26:90–99.
5. Joffre OP, Segura E, Savina A, Amigorena S. Cross-presentation by dendritic cells. *Nat Rev Immunol*. 2012;12(8):557–569.
6. Jongbloed SL, et al. Human CD141+ (BDCA-3)+ dendritic cells (DCs) represent a unique myeloid DC subset that cross-presents necrotic cell antigens. *J Exp Med*. 2010;207(6):1247–1260.
7. Crozat K, et al. The XC chemokine receptor 1 is a conserved selective marker of mammalian cells homologous to mouse CD8alpha+ dendritic cells. *J Exp Med*. 2010;207(6):1283–1292.
8. Bachem A, et al. Superior antigen cross-presentation and XCR1 expression define human CD11c+CD141+ cells as homologues of mouse CD8+ dendritic cells. *J Exp Med*. 2010;207(6):1273–1281.
9. Chiang MC, et al. Differential uptake and cross-presentation of soluble and necrotic cell antigen by human DC subsets. *Eur J Immunol*. 2016;46(2):329–339.
10. Schulz O, et al. Toll-like receptor 3 promotes cross-priming to virus-infected cells. *Nature*. 2005;433(7028):887–892.
11. Kroczek RA, Henn V. The Role of XCR1 and its ligand XCL1 in antigen cross-presentation by murine and human dendritic cells. *Front Immunol*. 2012;3:14.
12. Caminschi I, et al. The dendritic cell subtype-restricted C-type lectin Clec9A is a target for vaccine enhancement. *Blood*. 2008;112(8):3264–3273.
13. Sancho D, et al. Tumor therapy in mice via antigen targeting to a novel, DC-restricted C-type lectin. *J Clin Invest*. 2008;118(6):2098–2110.
14. Huysamen C, Willment JA, Dennehy KM, Brown GD. CLEC9A is a novel activation C-type lectin-like receptor expressed on BDCA3+ dendritic cells and a subset of monocytes. *J Biol Chem*. 2008;283(24):16693–16701.
15. Sancho D, et al. Identification of a dendritic cell receptor that couples sensing of necrosis to immunity. *Nature*. 2009;458(7240):899–903.
16. Zhang J-G, et al. The dendritic cell receptor Clec9A binds damaged cells via exposed actin filaments. *Immunity*. 2012;36(4):646–657.
17. Zelenay S, et al. The dendritic cell receptor DNGR-1 controls endocytic handling of necrotic cell antigens to favor cross-priming of CTLs in virus-infected mice. *J Clin Invest*. 2012;122(5):1615–1627.
18. Ahrens S, et al. F-Actin is an evolutionarily conserved damage-associated molecular pattern recognized by DNGR-1, a receptor for dead cells. *Immunity*. 2012;36(4):635–645.
19. Radford KJ, Caminschi I. New generation of dendritic cell vaccines. *Hum Vaccin Immunother*. 2013;9(2):259–264.
20. Broz ML, et al. Dissecting the tumor myeloid compartment reveals rare activating antigen-presenting cells critical for T cell immunity. *Cancer Cell*. 2014;26(5):638–652.
21. Sanchez-Paulete AR, et al. Cancer immunotherapy with immunomodulatory anti-CD137 and anti-PD-1 monoclonal antibodies requires BATF3-dependent dendritic cells. *Cancer Discovery*. 2016;6(1):71–79.
22. Tullett KM, Lahoud MH, Radford KJ. Harnessing human cross-presenting CLEC9AXCR1 dendritic cells for immunotherapy. *Front Immunol*. 2014;5:239.
23. Tacken PJ, et al. Effective induction of naive and recall T-cell responses by targeting antigen to human dendritic cells via a humanized anti-DC-SIGN antibody. *Blood*. 2005;106(4):1278–1285.
24. Klechevsky E, et al. Cross-priming CD8+ T cells by targeting antigens to human dendritic cells through DCIR. *Blood*. 2010;116(10):1685–1697.
25. Morse MA, et al. CDX-1307: a novel vaccine under study as treatment for muscle-invasive bladder cancer. *Expert Rev Vaccines*. 2011;10(6):733–742.
26. Schreibelt G, et al. The C-type lectin receptor CLEC9A mediates antigen uptake and (cross-)presentation by human blood BDCA3+ myeloid dendritic cells. *Blood*. 2012;119(10):2284–2292.
27. Hawiger D, et al. Dendritic cells induce peripheral T cell unresponsiveness under steady state conditions in vivo. *J Exp Med*. 2001;194(6):769–779.
28. Bonifaz LC, et al. In vivo targeting of antigens to maturing dendritic cells via the DEC-205 receptor improves T cell vaccination. *J Exp Med*. 2004;199(6):815–824.

29. Trumpfheller C, et al. Intensified and protective CD4+ T cell immunity in mice with anti-dendritic cell HIV gag fusion antibody vaccine. *J Exp Med*. 2006;203(3):607–617.

30. Dudziak D, et al. Differential antigen processing by dendritic cell subsets in vivo. *Science*. 2007;315(5808):107–111.

31. Flynn BJ, et al. Immunization with HIV Gag targeted to dendritic cells followed by recombinant New York vaccinia virus induces robust T-cell immunity in nonhuman primates. *Proc Natl Acad Sci U S A*. 2011;108(17):7131–7136.

32. Dhodapkar MV, et al. Induction of antigen-specific immunity with a vaccine targeting NY-ESO-1 to the dendritic cell receptor DEC-205. *Sci Transl Med*. 2014;6(232):232–251.

33. Cohn L, et al. Antigen delivery to early endosomes eliminates the superiority of human blood BDCA3+ dendritic cells at cross presentation. *J Exp Med*. 2013;210(5):1049–1063.

34. Kato M, et al. Expression of human DEC-205 (CD205) multilectin receptor on leukocytes. *Int Immunol*. 2006;18(6):857–869.

35. Lahoud MH, et al. Targeting antigen to mouse dendritic cells via Clec9A induces potent CD4 T cell responses biased toward a follicular helper phenotype. *J Immunol*. 2011;187(2):842–850.

36. Joffre OP, Sancho D, Zelenay S, Keller AM, Reis e Sousa C. Efficient and versatile manipulation of the peripheral CD4+ T-cell compartment by antigen targeting to DNGR-1/CLEC9A. *Eur J Immunol*. 2010;40(5):1255–1265.

37. Idoyaga J, et al. Comparable T helper 1 (Th1) and CD8 T-cell immunity by targeting HIV gag p24 to CD8 dendritic cells within antibodies to langerin, DEC205, and clec9a. *Proc Natl Acad Sci U S A*. 2011;108(6):2384–2389.

38. Kato Y, et al. Targeting antigen to Clec9A primes follicular Th cell memory responses capable of robust recall. *J Immunol*. 2015;195(3):1006–1014.

39. Iborra S, Izquierdo HM, Marinez-Lopez M, Blanco-Menendez N, Reis e Sousa C, Sancho D. The DC receptor DNGR-1 mediates cross-priming of CTLs during vaccinia virus infection in mice. *J Clin Invest*. 2012;122(5):1628–1643.

40. Li J, et al. Antibodies targeting Clec9A promote strong humoral immunity without adjuvant in mice and non-human primates. *Eur J Immunol*. 2015;45(3):854–864.

41. Corbett AJ, et al. Antigen delivery via two molecules on the CD8− dendritic cell subset induces humoral immunity in the absence of conventional "danger". *Eur J Immunol*. 2005;35(10):2815–2825.

42. Flinsenberg TW, et al. Cognate CD4 T-cell licensing of dendritic cells heralds anti-cytomegalovirus CD8 T-cell immunity after human allogeneic umbilical cord blood transplantation. *J Virol*. 2015;89(2):1058–1069.

43. Ding Y, et al. FLT3-ligand treatment of humanized mice results in the generation of large numbers of CD141+ and CD1c+ dendritic cells in vivo. *J Immunol*. 2014;192(4):1982–1989.

44. Newman R, et al. Modification of the Fc region of a primatized IgG antibody to human CD4 retains its ability to modulate CD4 receptors but does not deplete CD4(+) T cells in chimpanzees. *Clin Immunol*. 2001;98(2):164–174.

45. Reddy MP, et al. Eliminations of Fc receptor-dependent effector functions of a modified IgG4 monoclonal antobody to human CD4. *J Immunol*. 2000;164(4):1925–1933.

46. Tsuji T, et al. Antibody-targeted NY-ESO-1 to mannose receptor or DEC-205 in vitro elicits dual human CD8+ and CD4+ T cell responses with broad antigen specificity. *J Immunol*. 2011;186(2):1218–1227.

47. Bozzacco L, et al. DEC-205 receptor on dendritic cells mediates presentation of HIV gag protein to CD8+ T cells in a spectrum of human MHC I haplotypes. *Proc Natl Acad Sci U S A*. 2007;104(4):1289–1294.

48. Gurer C, et al. Targeting the nuclear antigen 1 of Epstein-Barr virus to the human endocytic receptor DEC-205 stimulates protective T-cell responses. *Blood*. 2008;112(4):1231–1239.

49. Chatterjee B, et al. Internalization and endosomal degradation of receptor-bound antigens regulate the efficiency of cross presentation by human dendritic cells. *Blood*. 2012;120(10):2011–2020.

50. Burgdorf S, Scholz C, Kautz A, Tampe R, Kurts C. Spatial and mechanistic separation of cross-presentation and endogenous antigen presentation. *Nat Immunol*. 2008;9(5):558–566.

51. Mahnke K, et al. The dendritic cell receptor for endocytosis, DEC-205, can recycle and enhance antigen presentation via major histocompatibility complex class II-positive lysosomal compartments. *J Cell Biol*. 2000;151(3):673–683.

52. Petzold C, Schallenberg S, Stern JN, Kretschmer K. Targeted antigen delivery to DEC-205(+) dendritic cells for tolerogenic vaccination. *Rev Diabet Stud*. 2012;9(4):305–318.

53. Spiering R, et al. DEC205+ dendritic cell-targeted tolerogenic vaccination promotes immune tolerance in experimental autoimmune arthritis. *J Immunol*. 2015;194(10):4804–4813.

54. Ring S, Maas M, Nettelbeck DM, Enk AH, Mahnke K. Targeting of autoantigens to DEC205(+) dendritic cells in vivo suppresses experimental allergic encephalomyelitis in mice. *J Immunol*. 2013;191(6):2938–2947.

55. Witmer-Pack MD, Swiggard WJ, Mirza A, Inaba K, Steinman RM. Tissue distribution of the DEC-205 protein that is detected by the monoclonal antibody NLDC-145. *Cell Immunol*. 1995;163(1):157–162.

56. Swiggard WJ, Mirza A, Nussenzweig M, Steinman RM. DEC-205, a 205-kDa protein abundant on mouse dendritic cells and thymic epithelium that is detected by the monoclonal antibodyNLDC-145: purification, characterization, and N-terminal amino acid sequence. *Cell Immunol*. 1995;165(2):302–311.

57. Hartung E, et al. Induction of potent CD8 T cell cytotoxicity by specific targeting of antigen to cross-presenting dendritic cells in vivo via murine or human XCR1. *J Immunol*. 2015;194(3):1069–1079.

58. Fossum E, et al. Vaccine molecules targeting Xcr1 on cross-presenting DCs induce protective CD8+ T-cell responses against influenza virus. *Eur J Immunol*. 2015;45(2):624–635.

59. Kontermann R, Duebel S, eds. *Antibody Engineering*. Vol. 1. Berlin/Heidelberg, Germany: Springer-Verlag; 2010.

60. Harding FA, Stickler MM, Razo J, DuBridge RB. The immunogenicity of humanized and fully human antibodies. *mAbs*. 2010;2(3):256–265.

61. Hersey P, Gallagher S. A focus on PD-L1 in human melanoma. *Clin Cancer Res*. 2013;19(3):514–516.

62. Topalian SL, Drake CG, Pardoll DM. Immune checkpoint blockade: a common denominator approach to cancer therapy. *Cancer Cell*. 2015;27(4):450–461.

63. Lahoud MH, et al. DEC-205 is a cell surface receptor for CpG oligonucleotides. *Proc Natl Acad Sci U S A*. 2012;109(40):16270–16275.

64. Vremec D, Pooley J, Hochrein H, Wu L, Shortman K. CD4 and CD8 expression by dendritic cell subtypes in mouse thymus and spleen. *J Immunol*. 2000;164(6):2978–2986.